SUPPLEMENTARY DATA

Participant Eligibility and Exclusion Criteria

Eligibility criteria for the T1D participants included age of onset of T1D after 6 months, positive islet cell autoantibody testing (GAD65, ICA512, and mIAA) if onset was before 12 months of age, and use of insulin for at least 1 month. Requirements for nondiabetic control subjects included HbA1c<6.0% (42 mmol/mol), fasting glucose < 110 mg/dL, and no history of abnormal glycemic control. Sibling control subjects of T1D participants were considered for inclusion in the control group if they had negative antibody testing within the prior year. Exclusions for both groups included genetic or mental disorders that could impair neurological development, history of intellectual disability or significant learning disabilities, psychiatric treatment, premature birth (<=34 weeks gestation), low birth weight (<=2,000 g), and magnetic resonance imaging (MRI) contraindications (e.g., metal implants).

Out of the main cohort of participants, for whom rsfMRI data was collected, 83 participants were selected based upon following two data-usability criteria. First, after preprocessing, participants with a minimum of 4 min of artifact free rsfMRI data (1) were included in further analysis. Second, after scrubbing, participants with a mean frame-wise displacement (FD) of greater than 0.2mm were excluded for further analysis (see preprocessing section below).

rsfMRI Data Preprocessing

Standard functional magnetic resonance imaging (fMRI) and rsfMRI preprocessing were performed using the Configurable Pipeline for the Analysis of Connectomes (C-PAC version 0.3.4; http://fcp-indi.github.io/docs/user/index.html). The C-PAC is an open-source software pipeline for automated preprocessing and analysis of resting-state fMRI data. C-PAC builds upon a robust set of existing software packages including AFNI, FSL, and ANTS, and makes it easy for both novice users and experts to explore their data using a wide array of analytic tools. C-PAC is being widely used as a state-of-the-art solution to exploring functional connectome data from thousands of subjects (e.g., 1000 Functional Connectomes project).

Anatomical preprocessing: registration

To compare brain activations across participants (and between groups) individual functional and anatomical MR images were transformed to a common MNI 152 brain template that is maintained by the Montreal Neurological Institute (MNI; (2)). We used the Advanced Normalization Tool (ANTS) for registering images, as it has been shown to outperform other methods (3). Registration involves a three-step process – (1) individual participant's anatomical images are first transformed to match the common template; followed by (2) registering individual participant's functional data to own transformed anatomical image; and finally (3) functional derivative files are transformed to the common template.

Anatomical preprocessing: anatomical tissue segmentation

The C-PAC uses FMRIB's Automated Segmentation Tool (FAST; http://fsl.fmrib.ox.ac.uk/fsl/fslwiki/FAST) to automatically segment brain images into white matter, gray matter, and CSF. This is done using probability maps that contain information about the likelihood that a given voxel will be of a particular tissue type (4). The default tissue probability maps (referred to as Prior Probability Maps) used during segmentation are based on information from a large number of brains, and are based on the priors distributed with FSL and are included in the "Image Resource Files" package downloaded during installation.

SUPPLEMENTARY DATA

Functional preprocessing: nuisance signal regression

FMRI preprocessing included discarding first 10 volumes (or TRs) of data for signal stabilization, slice timing correction, motion correction (FSL MCFLIRT), skull stripping (FSL BET), grand mean scaling, spatial smoothing (FWHM 4mm) and temporal band-pass filter (0.01 Hz < f < 0.1 Hz). Additionally, nuisance signal correction was done on the data by regressing out (1) linear and quadratic trends; (2) mean time-series from the white matter (WM) and the cerebrospinal fluid (CSF); (3) 24 motion parameters obtained by motion correction (the 6 motion parameters of the current volume and the preceding volume, plus each of these values squared.); and (4) signals extracted using the CompCor algorithm (5). The CompCor algorithm uses principal component analysis (PCA) to characterize the time series data from the noise ROIs (WM and CSF). Significant principal components are then introduced as covariates in a general linear model (GLM) as an estimate of the physiological noise signal space. We used 5 components for CompCor based nuisance regression (5).

Functional preprocessing: Scrubbing

To ensure that group differences in RSFC are not influenced by spurious motion-related noise, scrubbing was done (6, 7). This scrubbing procedure includes "censuring" data points where significant movement occurred. Two measures were used to identify the volumes contaminated by excessive motion – frame-wise displacement (FD) and DVARS (D referring to temporal derivative of time course, VARS referring to RMS variance over voxels). The FD is calculated from derivatives of the six rigid-body realignment parameters estimated during standard volume realignment, and is a compressed single index of the six realignment parameters. The DVARS is calculated by first differentiating the volumetric time series and then calculating the RMS signal change over the whole brain. This measure indexes the change rate of BOLD signal across the entire brain at each frame of data or, in other words, how much the intensity of a brain image changes relative to the previous time point.

Together, these two measures capture the head displacements and the brain-wide BOLD signal displacements from volume to volume over all voxels within the brain (6).

After calculating FD and DVARS, thresholds can be applied to censor the data. Data driven thresholds (i.e., 75th percentile + 1.5 times the Inter Quartile Range) for FD and DVARS were selected using the fsl_motion_outliers tool (part of FSL). In addition, to accommodate temporal smoothing of BOLD data, we also marked 1 back and 2 forward frames from any marked frames where FD/DVARS threshold was crossed. No group differences were observed for (a) total number of outlier frames; (b) mean FD after scrubbing; and (c) duration of "clean" (after scrubbing) resting state data (see Table 1, manuscript).

Seed-based connectivity analysis

For seed-based connectivity analysis, we chose brain regions previously shown to be associated with glycemic dysregulation in T1D. Specifically, a priori locations were chosen in the left prefrontal cortex (MNI coordinates: -28, 40, 33) and right lingual gyrus (MNI coordinates: 14, -53, 0). A 6 mm sphere was created around the left prefrontal cortex and right lingual gyrus location. Extracted time-series of these two locations were modeled with GLM analysis using the FMRI Expert Analysis Tool (FEAT) to estimate the ROI connectivity maps for each subject. For the group-level comparisons, age, sex and data-acquisition site location was used a covariates of no interest. Group-level maps were cluster-corrected using standard value of Z=2.3 and FWE $p<0.05$.

SUPPLEMENTARY DATA

Within-network connectivity analysis

Using group-ICA and dual regression (8), we examined short-range (or within network) RSFC differences associated with T1D within large-scale brain networks. This analysis involves three main steps. First, data-driven spatial maps are created by running group-ICA (8) on temporally concatenated data from equal number of participants from both groups. To reduce the bias from the fact that number of participants in T1D group was twice as much as in the ND control group, we randomly selected 26 participants from T1D group to match the number of participants in the ND control group. Analysis was carried out using Probabilistic Independent Component Analysis (9) as implemented in MELODIC (Multivariate Exploratory Linear Decomposition into Independent Components) Version 3.14, part of FSL (FMRIB's Software Library, www.fmrib.ox.ac.uk/fsl). Pre-processed data were whitened and projected into a 66-dimensional subspace using probabilistic Principal Component Analysis where the number of dimensions was estimated using the Laplace approximation to the Bayesian evidence of the model order (9). The whitened observations were decomposed into sets of vectors which describe signal variation across the temporal domain (time-courses), the session/subject domain and across the spatial domain (maps) by optimizing for non-Gaussian spatial source distributions using a fixed-point iteration technique (10) . Estimated Component maps were divided by the standard deviation of the residual noise and thresholded by fitting a mixture model to the histogram of intensity values (9).

Second, the group ICA components derived from step 1 are then dual-regressed into the subject space for all the 83 subjects. This dual regression includes two steps – first temporal regression and then spatial regression to estimate subject-specific spatial maps for each component (8). Dual regression tool provided by FSL was used for this step.

Third, for selected a priori components (as described in main text), we examined within-network connectivity differences in two large-brain brain networks (dorsal attention network and ventral attention network) associated with T1D. Group-level analysis was performed by contrasting subject-specific spatial maps for the two large-scale networks, while controlling for age, sex, and data-acquisition site location. To determine significant group differences, FSL's randomise permutation tool was used that uses a threshold-free cluster enhancement (TFCE) procedure at a family-wise error ($p < 0.05$) with 10,000 iterations (11).

Between-network connectivity analysis

In addition to within network connectivity, we also examined RSFC differences associated with T1D *between* large-scale brain networks. As none of the previous studies have examined such between-network long-range connectivity in individuals with T1D, as an exploratory analysis, we examined differences across all the networks identified by the probabilistic group ICA (see section 3 above). FSLNets v0.6 was used to perform this analysis. Component time series was estimated, for each of the 66 IC, using dual-regression stage-1. In dual-regression stage-1, full set of ICA maps was used as spatial regressors against the full time series data, estimating one time series for each ICA map and overall 66 time series for each subject (12, 13). Out of the 66 components derived from the Probabilistic group ICA, 18 were deemed noisy (or "bad") based on their topographic location (e.g., in white matter or outside of the brain) and power spectra (e.g., flat power spectra depicting white noise; See Figure S2). Network matrices (aka netmats) were then derived from the leftover 48, putatively neuronal, component time series. For each subject, 48 component time series were fed into network modeling, creating a 48 x 48 matrix of connectivity estimates. Network modeling was carried out using the FSLNets toolbox (http:// fsl.fmrib.ox.ac.uk/fsl/fslwiki/FSLNets). For network modeling, we used partial temporal

correlation between components' time series, which estimates connection strengths more accurately than is achieved by full correlation (14). To improve the stability of the estimates of partial correlation coefficients, a small amount of L2 regularization is applied (setting rho = 0.01 in the Ridge Regression netmats option in FSLNets). Netmat values were converted from Pearson correlation scores (r values) into z statistics with Fisher's transformation. Averaged netmat along with "good" or neuronal ICs are shown in Figure S1. After estimating this z transformed netmat values for each participant, group-wise differences were estimated (while controlling for age, sex, and data-acquisition site location) using FSL's randomize tool with TFCE. The false discovery rate (FDR) was use to correct for 1128 (i.e., 48 x 47/2) tests..

SUPPLEMENTARY DATA

Supplementary Figure S1. Shows average connectivity between different ICs across all participants. Top parts of the figure shows associated spatial maps of different ICs. The bottom part shows connectivity matrix between all 48 ICs, with upper diagonal depicting partial correlation and lower diagonal depicting full correlation values.

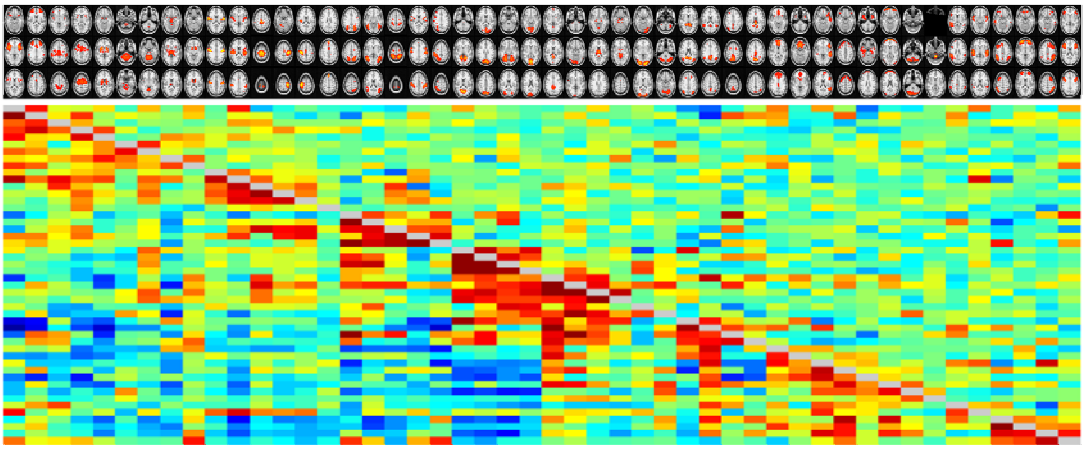

SUPPLEMENTARY DATA

Supplementary Figure S2. Shows IC components deemed noisy for the between-network analysis. (A) Denotes their spatial profile and (B-C) depicts the spectral profile for each of the noisy IC component. As evidence from the power spectral profile, the spectral power for noisy components is either flat or increasing with higher frequencies. Note as the data were band-pass filtered for 0.01-0.1Hz, the drop after 0.1Hz is due to filtering.

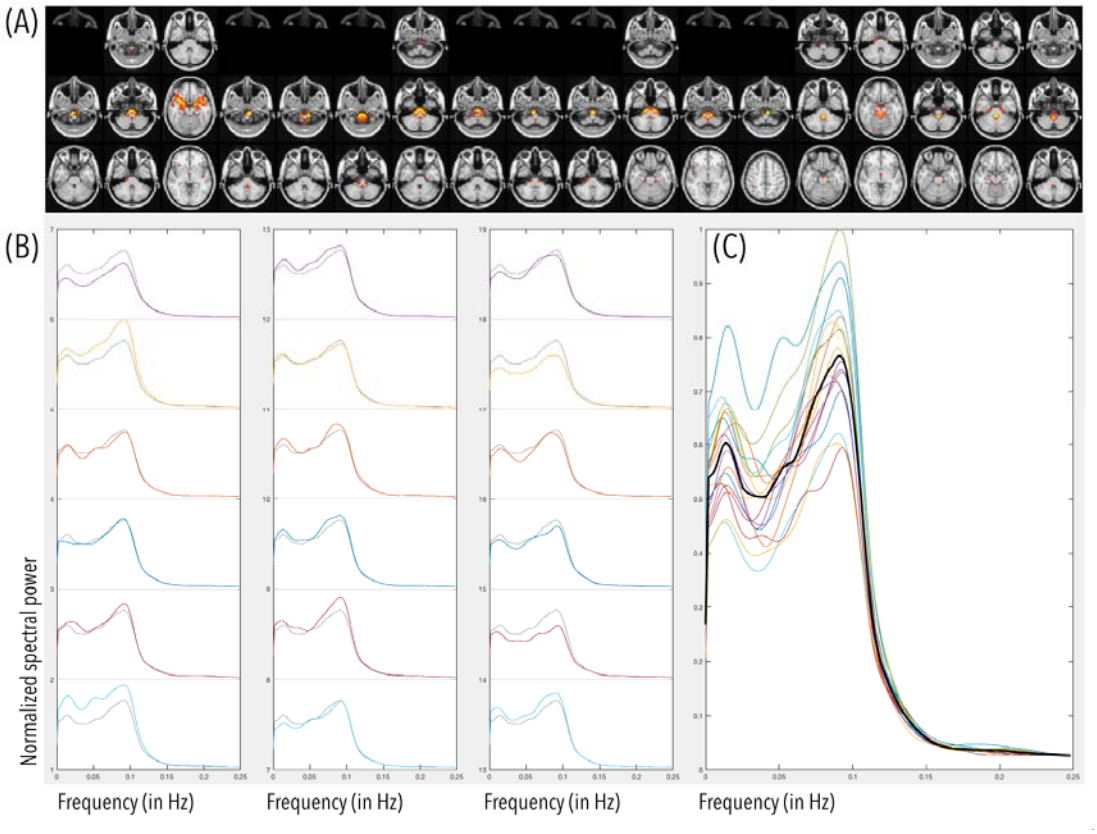

SUPPLEMENTARY DATA

References:

1. Satterthwaite TD, et al. (2013) An improved framework for confound regression and filtering for control of motion artifact in the preprocessing of resting-state functional connectivity data. *NeuroImage* 64:240–256.

2. Dabelea D, et al. (2014) Prevalence of type 1 and type 2 diabetes among children and adolescents from 2001 to 2009. *JAMA* 311(17):1778–1786.

3. Klein A, et al. (2010) Evaluation of volume-based and surface-based brain image registration methods. *NeuroImage* 51(1):214–220.

4. Zhang Y, Brady M, Smith S (2001) Segmentation of brain MR images through a hidden Markov random field model and the expectation-maximization algorithm. *IEEE Trans Med Imaging* 20(1):45–57.

5. Behzadi Y, Restom K, Liau J, Liu TT (2007) A component based noise correction method (CompCor) for BOLD and perfusion based fMRI. *NeuroImage* 37(1):90–101.

6. Power JD, Barnes KA, Snyder AZ, Schlaggar BL, Petersen SE (2012) Spurious but systematic correlations in functional connectivity MRI networks arise from subject motion. *NeuroImage* 59(3):2142–2154.

7. Power JD, Schlaggar BL, Petersen SE (2015) Recent progress and outstanding issues in motion correction in resting state fMRI. *NeuroImage* 105:536–551.

8. Filippini N, et al. (2009) Distinct patterns of brain activity in young carriers of the APOE- 4 allele. *Proceedings of the National Academy of Sciences* 106(17):7209–7214.

9. Beckmann CF, Smith SM (2004) Probabilistic independent component analysis for functional magnetic resonance imaging. *IEEE Trans Med Imaging* 23(2):137–152.

10. Hyvärinen A (1999) Fast and robust fixed-point algorithms for independent component analysis. *IEEE Trans Neural Netw* 10(3):626–634.

11. Winkler AM, Ridgway GR, Webster MA, Smith SM, Nichols TE (2014) Permutation inference for the general linear model. *NeuroImage*. doi:10.1016/j.neuroimage.2014.01.060.

12. Smith SM, et al. (2015) A positive-negative mode of population covariation links brain connectivity, demographics and behavior. *Nat Neurosci* 18(11):1565–1567.

13. Filippini N, et al. (2009) Distinct patterns of brain activity in young carriers of the APOE-epsilon4 allele. *Proceedings of the National Academy of Sciences* 106(17):7209–7214.

14. Marrelec G, et al. (2006) Partial correlation for functional brain interactivity investigation in functional MRI. *NeuroImage* 32(1):228–237.